

NUMERICAL SIMULATION OF QUASI-LINEAR CONVECTIVE SYSTEMS IN HETEROGENEOUS MESOSCALE ENVIRONMENTS

Dustan M. Wheatley and Robert J. Trapp
Purdue University, West Lafayette, IN

1. Introduction

An important unresolved issue in severe weather research is the relationship between quasi-linear convective systems (QLCSs) such as squall lines and bow echoes and the inhomogeneous environments within which they evolve. Idealized numerical simulations produce apparently severe QLCSs in the absence of environmental inhomogeneities. Nevertheless, recent observational studies (e.g., Klimowski et al. 2000; Pryzbylinski et al. 2000; Schmocker et al. 2000) suggest that preexisting thermal boundaries and/or isolated thunderstorms cells in advance of QLCSs are general conditions leading to the occurrence of severe weather.

To date, evidence to support this argument has come only in the form of incomplete observational data. Alternatively, predicted model fields are fully three-dimensional and “complete” in all variables, but numerical studies of QLCSs are still limited by the use of environments that are horizontally homogeneous, despite growth in computing power and the development of next-generation mesoscale forecast models. The primary objective of this study, therefore, is to perform “realistic” (i.e., real-data) numerical simulations of QLCSs, emphasizing the role of mesoscale variability in enhancing QLCS severity.

2. Methodology

2.1 Modeling approach

The fully compressible, Euler nonhydrostatic Advanced Research WRF (WRF-ARW) Version 2 is used to perform real-data numerical simulations of observed severe QLCSs. The initial conditions for real-data cases are supplied

by the 40 km ETA analysis, with boundary conditions updated on a 3-h interval using the ETA model forecasts. The model is integrated in time using two-way interactive grid nesting to resolve convective scales [$O(1\text{ km})$]. A more complete description of WRF configuration is discussed on a case-by-case basis.

Through analysis of real-data simulations of severe QLCSs, the objectives herein are to: 1) identify the various environmental features (including, but not limited to, preexisting surface boundaries and/or isolated thunderstorm cells) that modify structure and evolution of simulated QLCSs, and quantify their characteristics; 2) determine the role of such interactions in enhancing QLCS severity, and how it differs in homogeneous versus inhomogeneous scenarios.

2.1 Quantifying the spatial scales of mesoscale heterogeneity

Ultimately, we shall determine the horizontal spatial scales of mesoscale heterogeneity present in the near environments of simulated QLCSs. As a first effort, we have used the two-dimensional discrete Fourier transform to determine the spectral coefficients of equivalent potential temperature fields (which couple the moisture content and temperature of the air) on the simulations’ high-resolution nested grids. For ease of interpretation, the spectra in two-dimensional wave space are collapsed to spectra in one-dimensional wave space by averaging over discrete annuli in the former (see Errico 1985). Preliminary results indicate that the one-dimensional spectra of equivalent potential temperature do not exhibit pronounced spectral peaks, but conform to a power law. Interpretation of these spectral slopes is ongoing, and is not reported here.

3. The bow echo on 6 July 2003

* *Corresponding author address:* Dustan M. Wheatley, Purdue Univ., Dept. of Earth and Atmospheric Sciences, West Lafayette, IN 47907-2051; email: dwheatle@purdue.edu

The bow echo of 6 July 2003, observed during BAMEX, is the subject of this part of the study. Throughout its lifetime, this convective system produced a number of high wind reports, and caused widespread F0-intensity wind damage across eastern Nebraska and western Iowa. It possessed a well-defined rear-inflow jet (RIJ) and also a wide variety of low-altitude mesovortices. A more complete comparison between the system- and subsystem-scale structures of the observed and simulated (see below) bow systems can be found in Wheatley and Trapp (2005).

3.1 WRF configuration

The WRF Version 2.1.2 modeling system is applied to a domain that covers the Great Plains, upper Midwest and the lower Ohio River. In this parent domain, the horizontal gridpoint spacing is 9 km. A subnest with a horizontal gridpoint spacing of 3 km is centered about Nebraska and western Iowa. The placement of this grid is chosen such that it covers the area of convective initiation, over south-central South Dakota and northeastern Nebraska. A subnest with 1-km horizontal gridpoint spacing is centered about eastern Nebraska and extreme western Iowa. The model grid includes 35 levels in the vertical, with monotonic stretching, increasing from 0.2 km gridpoint spacing near the surface to 1.5 km near the model top (i.e., the 50-hPa pressure surface). The model is initialized at 0000 UTC 5 July 2003 (as described above), approximately 18 h before convective initiation.

3.2 Mesoscale heterogeneity in the simulated atmosphere

At approximately 0130 UTC, several isolated convective cells initiate over extreme southeastern South Dakota, as evidenced by the 40-dBZ simulated radar reflectivity contour (Fig. 1a). The main convective line is located several tens of kilometers upwind of this region. By 0300 UTC, these convective cells and associated cold surface outflow have begun to interact with the northern end of the main convective line (Fig. 1b). An equivalent potential temperature gradient of approximately 10 K exists across the boundary. This bow echo-

boundary interaction is the subject of the next section.

3.3 The effect of mesoscale heterogeneity on the developmental history of MV

MV is one of a number of low-level mesovortices that is well formed during the mature stage of the simulated bow echo (for reference, see Figs. 1 or 2), and its interaction with the aforementioned cold surface outflow is preliminarily analyzed below.

At 0253 UTC, MV is manifested as a vertical vorticity maximum within an elongated region of vertical vorticity along the northern end of the system's leading edge (Fig. 2a-b). The vorticity maximum (approximately 0.01 s^{-1}) associated with MV is located just on the warm-air side of a thermal boundary oriented in the across-line direction. The intersection of the system-scale cold pool and the thermal boundary produces a focused region of enhanced low-level convergence (not shown). There is a matched response in the vertical rate of change of vertical velocity (hereafter, $\partial w/\partial z$) in the near-surface layer (Fig. 2b).

Over the next few minutes, in a storm-relative framework, the boundary moves toward the south-southeast. By 0256 UTC, the local maximum in the $\partial w/\partial z$ field associated with the boundary spatially corresponds with MV (Fig. 2c-d), thereby promoting the stretching and subsequent amplification of *preexisting* vertical vorticity (as supported by trajectory calculations; see below). This process of mesovortex intensification continues through 0303 UTC (Fig. 2e-f), after which mesovortex strength has increased by nearly 50%, to nearly 0.03 s^{-1} .

To better understand the nature of this bow echo-boundary interaction, at 0303 UTC, around the time of peak mesovortex intensity, backward trajectories were calculated for parcels spaced every 1 km within a cubic region encompassing MV. The upper bound for this cubic region is the model sigma level at approximately 1 km AGL. Parcels flowing into this subspace originate from the inflow, behind the gust front, and behind the boundary. For parcels that originate behind the gust front, analysis of the vorticity equation shows that significant vertical vorticity is generated as horizontal vorticity is tilted in descending air (Figs. 3a). (Parcel heights in Fig. 4a are with respect to mean sea level, from

which one should subtract an average terrain height of ~0.4-0.5 km to arrive at parcel heights with respect to ground level.). Instantaneous fields reveal that the tilting process is largely inoperable in the vicinity of the bow echo-boundary interaction, which is confirmed by a forcing analysis for parcels that originate behind the boundary (Figs. 3b). Parcels flowing along the boundary, which is associated with a small amount of preexisting vertical vorticity, encounter a focused region of rising air near the bow echo-boundary interaction and undergo significant stretching of vertical vorticity. Similarly, for near-surface parcels originating in the inflow, forcing analysis show that significant vertical vorticity is generated through the stretching of absolute vertical vorticity (Fig. 3c).

While significant, the bow echo-boundary interaction described above is a relatively short-lived process. Beyond 0303 UTC, MV's eastern flank still resides in the gradient of $\partial w/\partial z$ associated with the boundary, but the $\partial w/\partial z$ maximum has moved beyond the center of circulation, which is increasingly dislocated from the leading edge of the gust front (not shown).

Taken as a whole, these results strongly suggest that the effect of the boundary is necessary (but not sufficient) for the later-stage development of MV.

4. The squall-line bow echo on 24 October 2001

The squall-line bow echo on 24 October 2001 is the subject of this part of the study. During this event, low-altitude mesovortices were host to 30 tornadoes across Indiana, Ohio and Michigan. The National Weather Service for this event also logged numerous high wind reports. Occurring in October, this event is a nice example of a severe bow echo forced by a dynamic pattern more typical of cool-season months. The preliminary results of a real-data numerical simulation of this bow-echo event are presented.

4.1 WRF configuration

The WRF Version 2.1.2 modeling system is applied to a domain that covers the eastern one-half of the conterminous United States. In this parent domain, the horizontal gridpoint spacing is 9 km. A subnest with a horizontal gridpoint

spacing of 3 km is centered about Indiana and Michigan, while a subnest with 1-km horizontal gridpoint spacing is centered about north-central Indiana and southern Michigan. The placement of the latter grid is chosen such that it covers the area of embedded bowing segments. The model grid includes 35 levels in the vertical, with monotonic stretching, increasing from 0.2 km gridpoint spacing near the surface to 1.5 km near the model top (i.e., the 50-hPa pressure surface). The model is initialized at 0000 UTC 24 October 2001, approximately 12-24 h before convective initiation.

4.2 System-scale structure

Comparable to the observed severe squall-line bow echo (Fig. 4e-h), the simulated squall-line bow echo has a structure and evolution described as follows: By 1800 UTC, convective cells associated with a strong, pre-frontal convergence line organize into a linear convective system over central Illinois and southeastern Missouri (not shown). Around 2200 UTC, this main convective line develops a pronounced bowing segment over north-central Indiana and southern Michigan (Fig. 4c). At this time, the main convective line extends from southern Michigan southwestward over northeastern Arkansas, as evidenced by a continuous line of simulated radar reflectivity in excess of 35 dBZ. It should be noted that the timing of the simulated squall line, though, lags the observed system by about 1 h.

4.3 Comments on this simulation

A number of low-level mesovortices can be found along-line throughout the period 2100 UTC 24 - 0000 UTC 25 October 2001 (Fig. 5). At 2300 UTC, maximum vertical vorticities associated with two mesovortices exceed three times mesocyclone-scale vorticity (not shown). Notably, these circulations grow in an environment that lacks any pronounced inhomogeneities, as gauged by the gradient of equivalent potential temperature on the lowest grid level (approximately 100 m AGL). These values nowhere exceed 1 K/km, except at the system's leading edge (Fig. 5).

These results strongly suggest that environmental heterogeneities may be sufficient,

but not necessary, for the development of severe weather within QLCSs.

5. Summary and discussion

Preliminary results from real-data numerical simulations of the 24 October 2001 and 6 July 2003 bow echo events over eastern Nebraska/western Iowa and north-central Indiana/southern Michigan, respectively, have been presented. Predicted model fields from the real-data numerical simulation of the 6 July 2003 bow echo event evidence the role of preexisting surface boundaries in enhancing QLCS severity. In this case, a focused region of enhanced convergence associated with the area of bow echo-boundary interaction amplifies vertical vorticity (i.e., the low-level mesovortex) through vertical vortex stretching. Time series of the time-integrated contributions to vertical vorticity from tilting and stretching show that the tilting process is negligible for parcels flowing along the boundary into the updraft.

Clearly, such an external boundary is not a necessary condition for severe weather production within the simulated QLCSs. The squall-line bow echo of 24 October 2001 evolves within a quasi-homogeneous environment, and low-level mesovortices within the bowing segments achieve strengths greater than three times mesocyclone-scale vorticity (relatively stronger than all of the low-level mesovortices within the simulated bow echo of 6 July 2003). Precisely, it can be said that a preexisting surface boundary appears to be a sufficient condition that leads to the occurrence of severe weather.

6. Future work

In an effort to generalize these results, the scope of this research project will be expanded to include consideration of 3-4 bow echo events. Other possible candidate events are the bow echoes on 5 May 1996 and 4 July 1999 and the squall-line bow echo of 10 April 2001. While 3-4 bow echo events are a limited sample, the above mentioned bow-echo events span a number of months and synoptic weather patterns, and should ultimately contribute to robustness of the results of this research project.

The next major step in this study will be the implementation of new ensemble filtering

software by the NCAR Data Assimilation Initiative (DAI), in conjunction with the WRF model. High-resolution observations (namely, radar data) will be assimilated into WRF, in both space and time, to reproduce variations in the near-storm environment. The use of a data assimilation system allows us to control the information flow into the model, and further test solution dependence on various environmental features.

Acknowledgments. This research was supported at Purdue University by the Bilsland Fellowship (DMW) and by the National Science Foundation under Grant ATM-023344 (RJT and DMW).

7. REFERENCES

- Errico, R. M., 1985: Spectra computed from a limited area grid. *Mon. Wea. Rev.*, **113**, 1554-1562.
- Klimowski, B. A., R. Przybylinski, G. Schmocker, and M. R. Hjelmfelt, 2000: Observations of the formation and early evolution of bow echoes. Preprints, *20th Conf. on Severe Local Storms*, Orlando, FL, Amer. Meteor. Soc., 44-47.
- Przybylinski, R. W., G. K. Schmocker, and Y.-J. Lin, 2000: A study of storm and vortex morphology during the 'intensifying stage' of severe wind mesoscale convective systems. Preprints, *20th Conf. on Severe Local Storms*, Orlando, FL, Amer. Meteor. Soc., 173-176.
- Schmocker, G. K., R. W. Przybylinski, and E. N. Rasmussen, 2000: The severe bow echo Event of 14 June 1998 over the mid-Mississippi Valley region: A case of vortex development near the intersection of a preexisting boundary and a convective line. Preprints, *20th Conf. on Severe Local Storms*, Orlando, FL, Amer. Meteor. Soc., 169-172.
- Trapp, R. J., and M. L. Weisman, 2003: Low level mesovortices within squall lines and bow echoes. Part II: Their genesis and implications. *Mon. Wea. Rev.*, **131**, 2804-2823.
- Wheatley, D. M., and R. J. Trapp, 2005: Real data numerical simulations of severe bow echoes observed during BAMEX. Preprints, *11th Conf. on Mesoscale Processes*, Albuquerque, NM, Amer. Meteor. Soc., 2M.5.

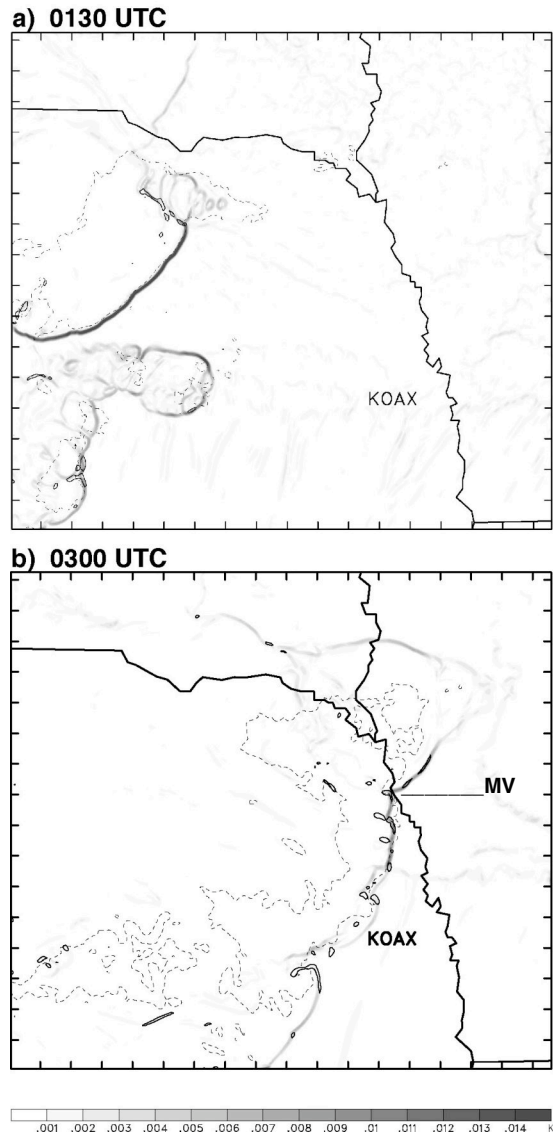


Fig. 1. Approximately 0.25-km AGL horizontal cross section at (a) 0130 and (b) 0300 UTC of the 40-dBZ contour (dashed line), 0.005-s⁻¹ vertical vorticity contour (solid line), and the magnitude of the horizontal gradient of the equivalent potential temperature (see color bar). Tick marks are plotted every 20 km.

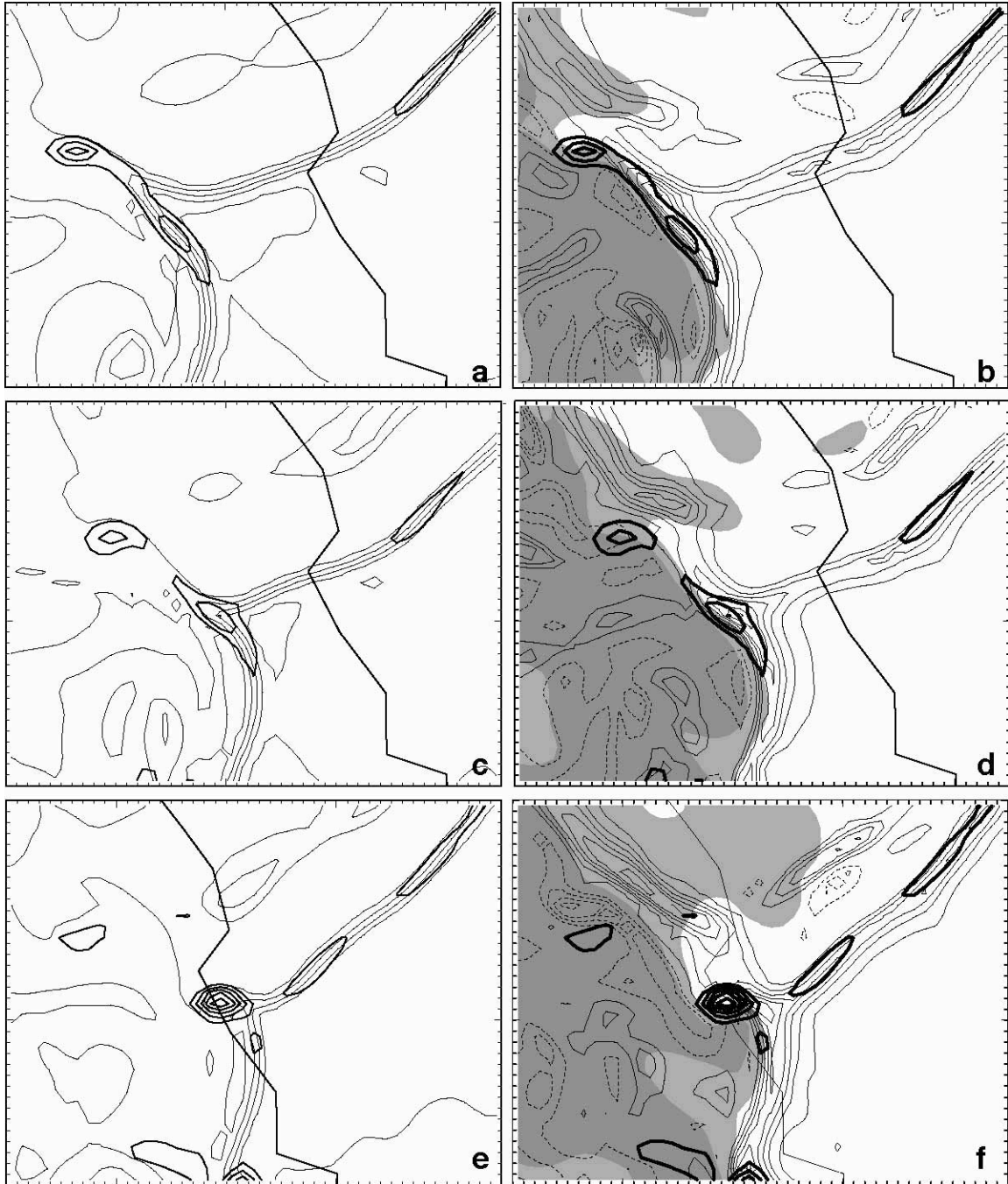


Fig. 2. Approximately 0.25-km AGL horizontal cross sections at (a) 0253, (c) 0256 and (e) 0303 UTC of equivalent potential temperature contours (thin solid lines; every 5 K); and at (b) 0253, (d) 0256 and (f) 0303 UTC of rainwater mixing ratio contours and $\partial w/\partial z$ contours (thin solid lines; every $250 \times 10^{-4} \text{ s}^{-1}$, with no zero contour and dashed negative contours). Rainwater mixing ratios between 1 and 3 g kg^{-1} are lightly shaded, with values greater than 3 g kg^{-1} darkly shaded. In (a)-(f), positive vertical vorticity contours are plotted every 0.005 s^{-1} (thick solid lines). Tick marks are plotted every 1 km.

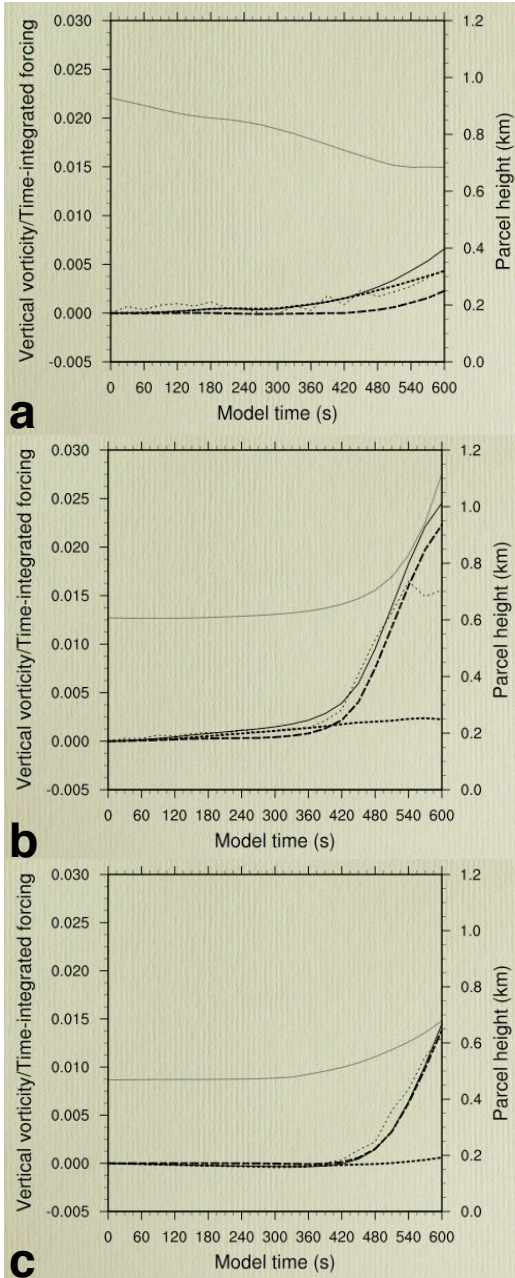


Fig. 3. Time series of parcel height (z , km) (thin solid line), vertical vorticity (ζ ; $\times 10^{-5} \text{ s}^{-1}$) (small dashed line), and the time integrated contributions to vertical vorticity (thick solid line) from the tilting (medium dashed line) and absolute vorticity-stretching terms (large dashed line) (s^{-1}) representative parcels originating (a) behind the gust front, (b) along the boundary, and in the (c) inflow.

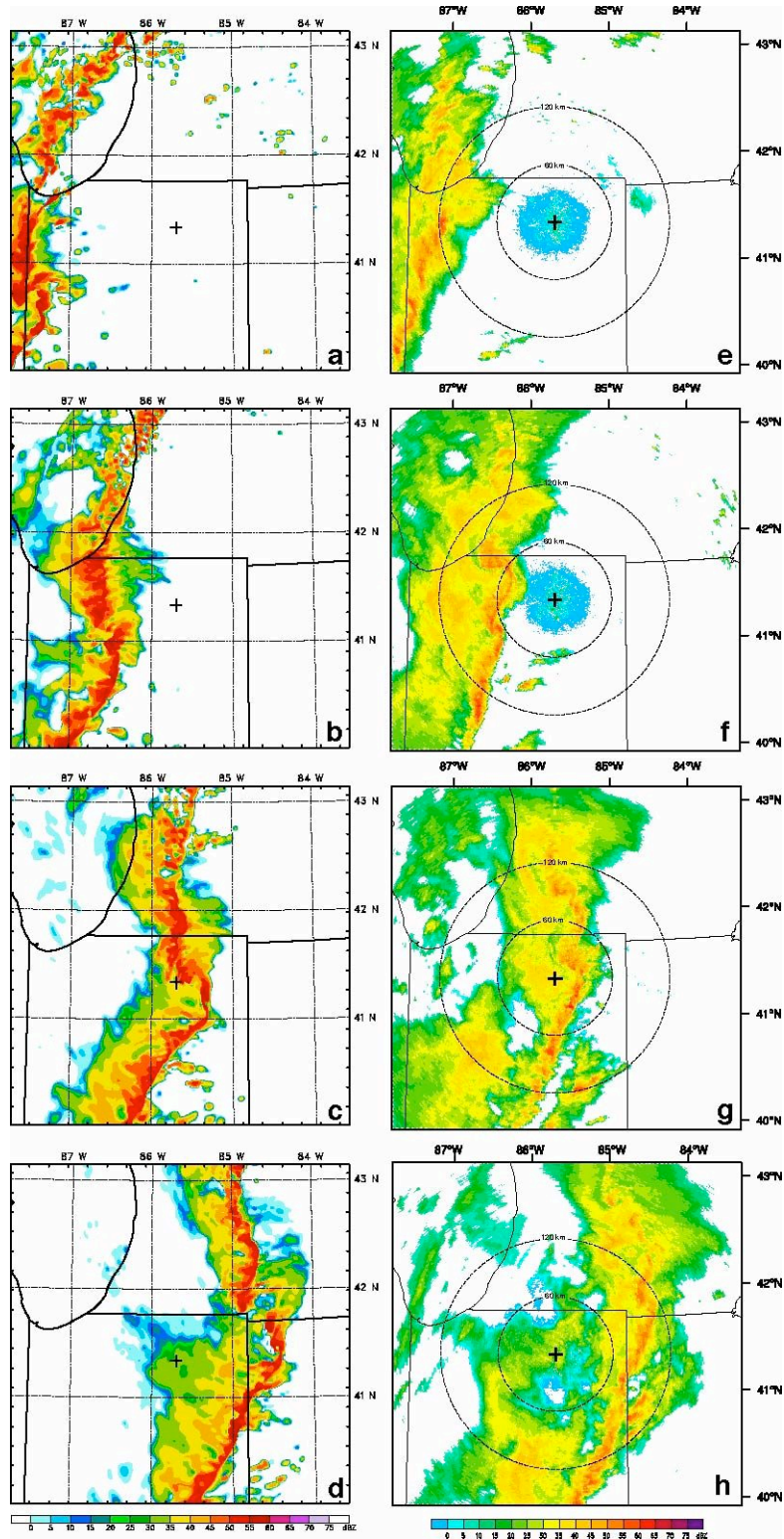


Fig. 4. Simulated radar reflectivity at (a) 2100, (b) 2200, (c) 2300 UTC 24 October 2001 and (d) 0000 UTC 25 October 2001, and single-Doppler reflectivity at (a) 2000, (b) 2100, (c) 2200 and (d) 2300 UTC 24 October 2001, of the squall-line bow echo over north-central Indiana and southern Michigan. **NOTE:** Due to timing differences between the simulated and observed systems, the row-wise comparisons [(a)-(e), (b)-(f), (c)-(g), and (d)-(h)] disagree by 1 h. For (a)-(d), tick marks are plotted every 20 km. For (e)-(h), a cross denotes the location of the KIWX WSR-88D, and range rings (dashed lines) are plotted every 60 km.

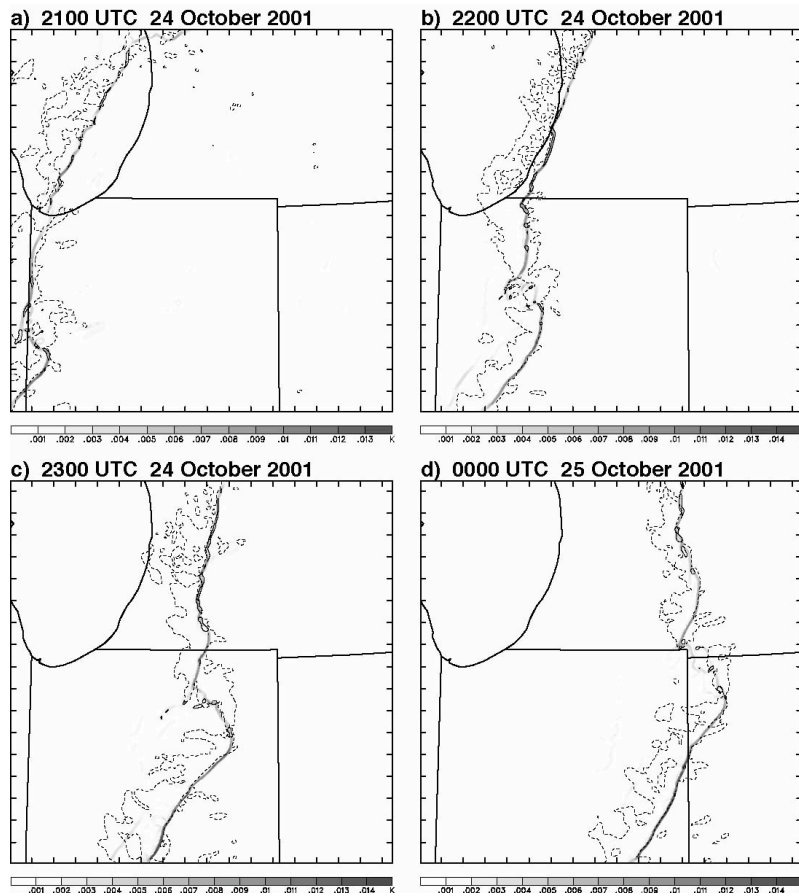


Fig. 5. Approximately 0.25-km AGL horizontal cross section at (a) 2100, (b) 2200, (c) 2300 UTC 24 October 2001, and d) 0000 UTC 25 October 2001 of the 40-dBZ contour (dashed line), 0.005-s⁻¹ vertical vorticity contour (solid line), and the horizontal gradient of the equivalent potential temperature (see color bar). Tick marks are plotted every 20 km.